CHEMISTRY
A European Journal

A Journal of
ChemPubSoc Europe

# Accepted Article

**Title:** Dual-selective and dual-enhanced SERS nanoprobes strategy for circulating hepatocellular carcinoma cells detection

**Authors:** Xiao Rui



**To be cited as:** *Chem. Eur. J.* 10.1002/chem.201801133

**Link to VoR:** http://dx.doi.org/10.1002/chem.201801133

Supported by
ACES

WILEY-VCH

10.1002/chem.201801133


WILEY-VCH

# Dual-selective and dual-enhanced SERS nanoprobes strategy for circulating hepatocellular carcinoma cells detection

Yuanfeng Pang,[a,1] Chongwen Wang[b,c,1], Rui Xiao*[b] and Zhiwei Sun*[a]

**Abstract:** The detection of hepatocellular carcinoma (HCC) circulating tumor cells (CTCs) from a blood sample can be a very powerful noninvasive approach for the early detection and therapy of liver cancer. However, the extremely rare cells in blood containing billions of other cells make the capture and identification of CTCs with sufficient sensitivity and specificity a real challenge. Here, a magnetically assisted surface-enhanced Raman scattering (SERS) biosensor for HCC CTCs detection is reported for the first time. The biosensor consists of two basic elements including an anti-ASGPR antibody-$Fe_3O_4$@Ag MNPs and an anti-GPC3 antibody-Au@Ag@DTNB NRs. According to the dual-selectivity of the anti-ASGPR and anti-GPC3 antibodies and the dual-enhancement SERS signal of the MNPs silver shell and the Au@Ag NRs SERS tags, a limit of detection of 1 cell/mL for HCC CTC in human peripheral blood samples with a linear relationship from 1 to 100 cells/ mL can be obtained. The system showed good performance in real serum which suggested they would be a promising tool for HCC clinical diagnosis.

## Introduction

Hepatocellular carcinoma (HCC) is one of the most common malignant tumors in the world and it remains the third leading cause of cancer-related deaths due to its aggressiveness and poor diagnosis. In the past few years, more and more attention has been focused on the circulating tumor cells (CTCs), which disengaged from the primary lesion and invade into the blood circulation. [1] CTCs are considered a good indicator for the presence of a primary tumor and a marker for understanding metastatic development. [2-4] Therefore, selective capture and accurate analysis of hepatocellular carcinoma tumor CTCs from a blood sample can be a very powerful noninvasive approach for the early detection of liver cancer. [5-7] However, CTCs circulate in peripheral blood at an extremely low frequency of 1–10 CTCs/ mL, so that the detection of CTCs within the large number of normal blood cells is still a big challenge. Therefore, a detection method with super-sensitivity and high-specificity is required for early diagnosis, metastasis investigation and treatment

Until now, many CTC isolation approaches have been established such as isolation by cell density, [8] by tumor cell size, [9] by flow cytometry. [10] During which, magnetic cell separation is thought to be highly specific and can be applied to separate CTCs from whole blood. Bead-based enrichment methods are divided into two categories: positive and negative enrichment. Positive enrichment refers to the method whereby tumor cells are separated directly in a magnetic field, such as the FDA approved anti-EpCAM antibodies modified immunomagnetic nanospheres(IMNs), CellSearch system, it can detect the EpCAM positive CTCs in 7.5 mL blood sample. Unfortunately, for HCC, although hepar is an epithelial organ, only 35% of the HCC cells from clinical sample of patients with hepatocarcinoma are EpCAM-positive, so that the CellSearch system may fail to capture and detect the HCC CTCs. Xu and coworkers [11] developed a HCC detection method by firstly inducing biotin to link the asialoglyco protein receptor (ASGPR) on the surface of HCC and then using the avidin-coated magnetic beads to capture the HCC cells. The operation was susceptible and the normal liver cells detachment by operation cannot be separated from HCC CTCs as ASGPR shows exclusively overexpression on the surface of human hepatocytes. In 2015, Shi and coworkers [12] reported a multifunctional biocompatible graphene oxide quantum dots (GOQDs) coated magnetic nanoplatform for the selective separation and diagnosis of HepG2 liver cancer tumor CTCs from infected blood with a capture efficiency of 91% in a 15 mL infected blood sample containing 10 cells/mL HepG2 tumor cells. However, the produce process of the graphene oxide quantum dots (GOQDs) coated $Fe_3O_4$ nanoplatforms was not easy to operate. Negative enrichment refers to removing non-specific cells such as leukocyte to purify target cells through a magnetic field. Recently, pang and co-workers have reported a negative enrichment cell sorting strategy using bio functionalized magnetic nanospheres to deplete leukocyte and isolate the HCC cells with leukocyte depletion efficiency up to 99.9%.[13] Here, for both positive and negative bead-based enrichment methods, the following CTC identification steps all depended on fluorescence-conjugated antibodies staining method, which required tedious complicated operations, suffered the auto-fluorescence background of blood and the presence of various fluorescent artifacts to decrease the sensitivity and narrow the linear range. Therefore, there is a large unmet need for suitable technologies that allow accurate intraoperative assessment of HCC cells, not only the precise separation method but also the simple detection method.

Surface-Enhanced Raman scattering (SERS) spectroscopy is an important analytical technique for biological sensing and trace analysis because of the enormous Raman enhancement. [14-16] The detection and identification of CTCs by SERS have recently attracted interest because of the potential application of this technology in single-cell detection. [17-20] During which, the SERS nanoparticles were used as tags to label the target CTCs. While, our group aimed to the alliance of the magnetic SERS enhancement substrate and the SERS tag for the target enrichment and detection, such as by using Ag-coated magnetic nanoparticles (MNPs) and Au or Au@Ag SERS tags for

[a] Prof. Dr. Z.W. Sun, Dr. Y.F. Pang.
Capital Medical University, Department of Toxicology,No.10 Xitoutiao, YouAn Men, Beijing 100069, (P.R China)
E-mail: ruixiao203@163.com
[b] Prof. Dr. R. Xiao, Dr. C.W. Wang.
Beijing Institute of Radiation Medicine, Beijing 100850, PR China.
[c] Dr. C.W. Wang.
College of Life Sciences & Bio-Engineering, Beijing University of Technology, Beijing 100124, (P.R China)

staphylococcus aureus [21] or carcinoembryonic antigen [22], the target can be captured by the Ag-coated MNPs and after labeled the SERS tags on the target, a dual SERS enhancement can be induced so that the detection sensitivity can be improved. Here in this study, a magnetically assisted SERS biosensor for HCC CTCs detection was proposed and constructed for the first time to the best of our knowledge. On the one hand, superparamagnetic $Fe_3O_4$@Ag MNPs were synthesized. The MNPs were utilized as the dual-functional substrate: 1. As CTCs enrichment platform 2. As the SERS signal amplification substrate. Subsequently, a silver-coated gold nanorods (Au@Ag NRs) were utilized as the SERS tag-substrate. 5, 5'-Dithiobis (2-nitrobenzoic acid) (DTNB) was linked on the surface of the Au@Ag NRs to form the SERS tag (Au@Ag@DTNB) considering the high SERS activity and conveniently conjugates with target recognition molecules (such as antibody or aptamer) of the DTNB molecule by using a previously reported method with some modifications. [23] On the other hand, to realize the specifically capture and recognition of HCC CTCs from the whole blood sample, specific antibodies for HCC cell surface antigens must be chosen and modified onto the surface of the capture and labelling nanospheres respectively. Recently, the asialoglyco protein receptor (ASGPR) and Glypican-3 (GPC3) have been used as the marker for the HCC cells as the ASGPR shows exclusively overexpression on the surface of human hepatocytes and GPC3 shows exclusively overexpression on the surface of the HCC cell line. [24-26] Until now, no biomarker has been certified as the "golden standard" for HCC recognition. In order to improve the veracity of our assay, an optimized combination of anti-ASGPR antibody and anti-GPC3 antibody was used to ensure that no target cell is missed. Through the optimization experiments in this paper, the anti-ASGPR antibody was functionalized on the $Fe_3O_4$@Ag MNPs to selectively capture the human hepatocytes in the blood sample (including the normal liver cells detachment by operation and HCC CTC); then, the anti-GPC3 antibody was functionalized on the Au@Ag@DTNB SERS tags to selectively label the HCC CTCs. Therefore, $Fe_3O_4$@Ag MNPs can be used for human hepatocytes (normal or HCC) capture (the first selectivity) and then only the HCC with GPC3 overexpression on the surface can be labeled by the SERS tags (the second selectivity). For the signal detection, this aggregation of the two nanospheres on the cell surface could induce the dual plasmonic coupling between the silver shell of MNPs and the Au@Ag of the tags except for the surface enhanced Raman scattering of the SERS tags itself, therefore, based on the dual signal enhancing strategies, the SERS signal of DTNB molecules located in the coupled plasmonic nanostructures could be significantly enhanced (Scheme 1). Coupled with dual-selectivity and dual-enhancement SERS signal, the HCC CTC detection can be expected with good sensitivity and specificity.

## Results and Discussion

### Synthetic route and the detection principle

Scheme 1a and 1b show the synthetic route of the anti-ASGPR conjugated $Fe_3O_4$@Ag MNPs and anti-GPC3 conjugated Au@Ag@DTNB respectively. As mentioned in the experiment method, the antibody can be linked on the surface of the nanoparticles through the amination reaction. Scheme 1c shows the HCC immunomagnetic separation, SERS tag labelling and Raman detection process. As shown in the scheme, anti-ASGPR-$Fe_3O_4$@Ag MNPs was used to capture and concentrate the target CTCs through immunomagnetic separation with the assistance of an external magnet instead of centrifugation. After separation, the anti-GPC3-Au@Ag@DTNB SERS tag can specifically label and report the existence of the target CTC. There was two obvious characteristics for our system: dual-selectivity and dual-enhancement SERS signal. For dual-selectivity: the first selectivity, only human hepatocytes (normal or HCC cancer cells) can be captured by the anti-ASGPR-$Fe_3O_4$@Ag MNPs; the second selectivity, only the HCC cells with GPC3 overexpressed can be labeled by the SERS tag and produce a SERS signal in the following detection. For dual-enhancement SERS signal: the Au@AgNRs could lead to a SERS enhancement nearly $6.6\times10^3$ in our previous report [21,22] and the "hotspots" in the adjacent slits between $Fe_3O_4$@Ag MNPs and the SERS tags will induce a further signal intensity enhancement of the Raman reporter molecules (DTNB) which located in the hotspot junction. There will be an advantage compared with the one-fold immunomagnetic separation and SERS tag labelling method reported previous. [31,32]

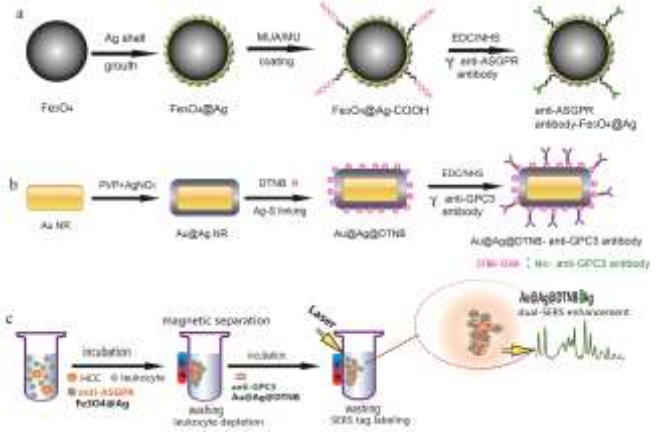


**Scheme 1.** Flowchart of HCC CTCs capture and detection using SERS. (a) synthesis of monodispersed silver-coated magnetic nanoparticles and their conjugation with anti-ASGPR antibody. (b) synthesis of core−shell plasmonic nanoparticles (Au@Ag@DTNB) and their conjugation with anti-GPC3 antibody. (c) schematic illustration of the operating principle for HCC CTCs detection.

### Characterization of the nanosphere couplings

The synthetic strategy and Transmission electron microscopy (TEM) images of the $Fe_3O_4$@Ag are shown in Figure 1a-c. After the formation of Ag shell, the mean diameter of the $Fe_3O_4$ MNPs increased from about 900 nm to nearly 1000 nm. Thus, the Ag shell thickness is approximately 50 nm. Figure 1d shows the SEM image of $Fe_3O_4$@Ag MNPs. The typical XRD patterns and

10.1002/chem.201801133



magnetic hysteresis curves of $Fe_3O_4$ and $Fe_3O_4$@Ag MNPs was shown in Figure. S1a-b. As shown in Figure. S1b, the saturation magnetization (MS) value of $Fe_3O_4$, $Fe_3O_4$@PEI and $Fe_3O_4$@Ag MNPs is 80, 65, and 50 emu $g^{-1}$ respectively, the $Fe_3O_4$@Ag MNPs retain major magnetic properties of the $Fe_3O_4$ core and also can be completely separated from the solution with 10 s when the magnetic field was applied (as shown in the photo).

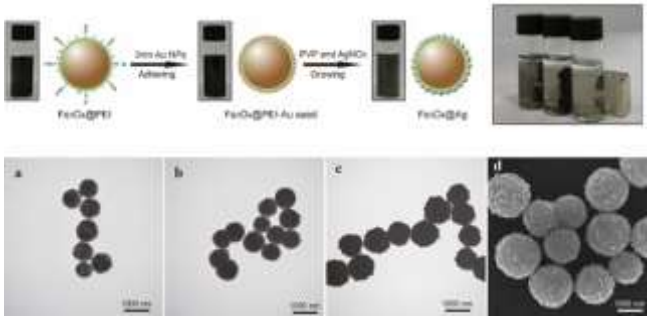

**Figure 1.** The synthetic strategy and Transmission electron microscopy (TEM) images of the $Fe_3O_4$@Ag MNPs. (a) $Fe_3O_4$@PEI MNPs; (b) $Fe_3O_4$@PEI@Au MNPs; (c,d) TEM and SEM of the $Fe_3O_4$@Ag MNPs.

The TEM image of the synthesized AuNRs(a), Au@Ag NRs with different Ag shell thickness (b=3.5 nm and c=5 nm) were shown in Figure 2a-c. According to the UV−vis spectra of the synthesized nanospheres (Figure 2d), the LSPR wavelength of the synthesized AuNRs(a) was 824nm. As the adjusting of the thickness of Ag shell can continuously tune the LSPR wavelength of the bimetallic NPs, it showed that the Au@Ag NRs with average size of 70 nm × 17.5 nm and with an average Ag shell thickness of 3.5 nm possess the LSPR wavelength which was consistent with the excitation wavelength of the laser (785 nm). From Figure 2e, the Au@Ag NRs with LSPR wavelength of 785nm will induce the strongest Raman signal (about 3 orders greater than the SERS intensity of DTNB modified AuNRs). The UV−vis spectra of the $Fe_3O_4$@Ag and $Fe_3O_4$ MNPs was also shown in Figure S8. To confirm that the anti-ASGPR and anti-GPC3 antibodies could be conjugated on the surface of $Fe_3O_4$@Ag MNPs and the Au@Ag@DTNB NRs, anti-ASGPR-$Fe_3O_4$@Ag MNPs and anti-GPC3-Au@Ag@DTNB NRs respectively reacted with FITC-labeled goat anti-mouse IgG. After 30 min incubation and washed 3 times with PBS, the fluorescence photos were recorded. Figure S2 showed the bright and fluorescence images of the antibody-$Fe_3O_4$@Ag (a,b) and antibody-Au@Ag@DTNB MNs (c,d) after reacted with FITC-labeled goat anti-mouse IgG. As shown in Figure S2, the green fluorescence of FITC on both $Fe_3O_4$@Ag MNPs and Au@Ag@DTNB NRs was obvious, which indicated that anti-ASGPR and anti-GPC3 antibodies were both successfully conjugated to the nanoparticles. The UV−vis spectra of the anti-ASGPR and anti-GPC3 antibodies before and after incubated with the $Fe_3O_4$@Ag and the SERS tags was shown in Figure S9, the decreasing of the intensity of 280 nm showed that the antibodies were modified on the surface of the nanoparticles from the solution.

To confirm the stability of the antibody-nanoparticles, we have also performed dynamic light scattering (DLS) measurement using a Malvern Zetasizer Nano instrument in solution phase. The DLS data was reported in TableS1. It indicated that the average size is about 900 nm for $Fe_3O_4$,1000 nm for antibody-$Fe_3O_4$@Ag nanoparticles, both hydrodynamic sizes changed little with half year storage time.

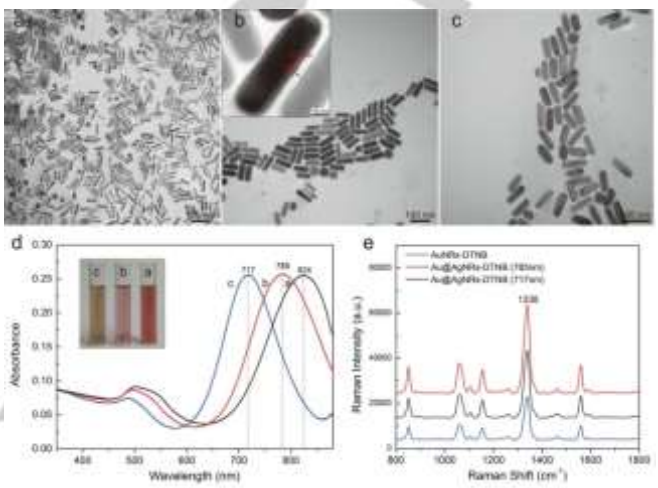


**Figure 2.** TEM images of (a) the synthesized AuNRs (b,c) the Au@Ag NR core−shell plasmonic nanoparticles with Ag shell thickness (b=3.5 nm and c=5 nm). (d) UV−visible spectra of the synthesized nanoparticles. (e) Raman intensity of AuNR@DTNB (LSPR =824 nm), Au@Ag@DTNB(LSPR =785 nm), and Au@Ag @DTNB(LSPR =717 nm) under the same conditions.

**Result of the optimization probes combination and the cell viability**

The capture efficiencies of the anti-ASGPR antibody-$Fe_3O_4$@Ag MNPs (sample 1) and anti-GPC3 antibody-$Fe_3O_4$@Ag MNPs (sample 2) with concentrations ranged from 0.1 mg/ mL to 0.6 mg/ mL was shown in Figure S3a. It showed that for both samples the capture efficiency increased with the increase of MNP s concentration. For sample 1, until the concentration reached 0.5 mg/mL, 98% of HepG2 cells were captured and then kept a platform even though the concentration increasing, for sample 2, 93% of HepG2 cells were captured. For the unmodified $Fe_3O_4$@Ag MNPs control (0.5 mg/mL), the cell capture efficiency is only less than 2% (induced by the nonspecific adsorption). Therefore, the capture efficiency for anti-ASGPR was a little better than anti-GPC3 and the 0.5 mg/mL can be selected as the optimized concentration of MNPs. Then, the SERS signals of the 4 kinds of combinations: anti-ASGPR-MNPs / anti-ASGPR-SERS tag (group1), anti-ASGPR -MNPs/anti-GPC3-SERS tag (group 2), anti-GPC3-MNPs/anti-GPC3-SERS tag (group 3), MNPs/SERS tag without antibody modified (control) were shown in Figure S3b. It showed that the group 2 can induce the stronger SERS signal compared to the group 1 and 3 in the same conditions. In our experiment, the

stronger SERS signal can induce higher sensitivity and lower detection limit. Therefore, we chose group 2 as the dual selectivity system. We prospect that the reason may be that there will be a competition if the same binding antibody was used in both capture and label processes as the binding site on the surface of the CTC was limited. Considering the better capture efficiency and sensitivity, the group 2 can be used for the optimized combination for CTC detection.

The separated cells by the anti-ASGPR-$Fe_3O_4$@Ag MNPs were stained by the Alexa488-GPC3 antibodies and then a drop of 1.5 μL was put on a glass slide for florescence observation. The result was shown in Figure 3a. Immunofluorescence characterization of the captured cells showed positive to the Alexa488-GPC3 antibodies so that it can be proved that cells captured by the MNPs were really the HepG2 cells. The Figure 3b showed the SEM of the HepG2 cell captured by the MNPs from the solution. It can be seen that the MNPs could be adsorbed to the surface of HepG2 cells well-proportioned. The result of the cell capture efficiency was given in Figure3c. The result of the cell viability was shown in Figure S4, it can be seen that the majority of the isolated cells showed green fluorescence, and the viability rate was calculated to be 92.5±1.3%, which indicated that most of the tumor cells remained viable after the isolation. Then, the isolated cancer cells were directly cultured without any handling. As shown in Figure S4, the cells adhered well, proliferated on the culture dish, and had successfully undergone multiple (>5) passages without detectable changes in morphology and behavior.

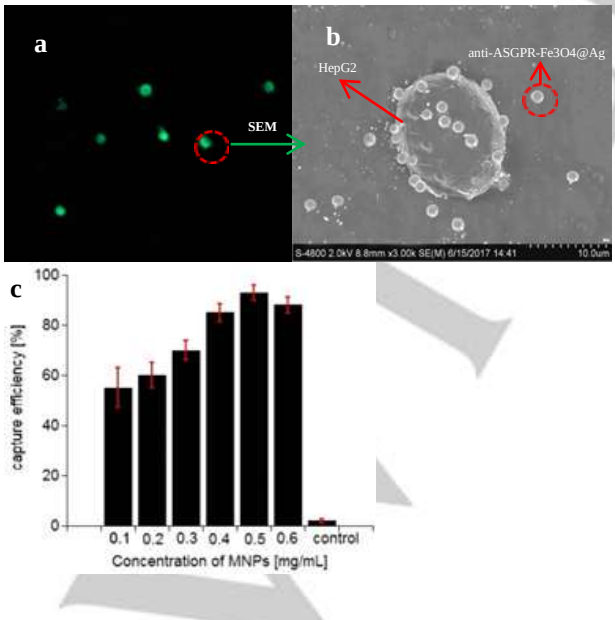


**Figure 3.** (a) Immunofluorescence characterization of the captured cells stained by the Alexa488-GPC3 antibodies,(b) the SEM of one of the HepG2 cells captured of figure 3a, (c) capture efficiencies of the MNPs with different concentrations to HepG2 cells.

### Sensitivity and specificity of the nanoparticle based magnetic Isolation and SERS detection

Here, to confirm the plasmonic coupling between the capturing substrates and the nanoprobes can improve the detection sensitivity, we did the control experiments. The anti-ASGPR-$Fe_3O_4$; anti-ASGPR-$Fe_3O_4$/anti-GPC3-Au@Ag@DTNB tags; anti-ASGPR-$Fe_3O_4$@Ag/anti-GPC3-Au@Ag@DTNB tags were respectively added to the HCC tumor cells sample solution in the same experiment conditions as mentioned in the manuscript and the SERS intensity was recorded. The result was given in the supplement information as FigureS.7. It showed that the SERS intensity by using $Fe_3O_4$@Ag substrate was increased about 3 orders compared with that by using $Fe_3O_4$ substrate in the same HCC concentration, which means that the sensitivity can be increased by the dual enhancement of SERS. The concentration of anti-GPC3 antibody conjugated Au@Ag@DTNB SERS tag was firstly optimized (FigureS.5) and the anti-ASGPR-$Fe_3O_4$@Ag MNPs and anti-GPC3-Au@Ag@DTNB SERS tag are utilized to capture and detect cancer cells in the peripheral human blood. Evaluations for the specificity and sensitivity of our magnetic SERS-active nanoparticles are operated on HepG2, MCF-7, and L-02 cells. Here, we define the LOD as the lowest cell concentration in the fitting line of SERS intensity versus cell concentration can be determined. Figure 4 shows the detection sensitivity and specificity of our system for HCC cells in the human peripheral blood. Figure 4a shows the SERS signals based on the main Raman peak (1331 $cm^{-1}$) of the SERS tag in the blood (1.0 mL, ~ 0.5 × $10^7$ WBCs) with different concentrations of HepG2 and we can see that the higher cell concentrations result in stronger SERS intensities in the range of 1-150 cells/mL. The fitting line inserted in the Figure 4a showed that the SERS intensity was linearly dependent on the HepG2 cell concentration ranging from 1 to 100 cells/mL with a $R^2$ of 0.99 and the sensitivity was similar to our previous reports using the semblable combination for bacteria detection with a LOD of 1 cells/mL, which was satisfied the standard of 1–10 CTCs/mL in patient blood samples. The SERS spectra taken from the SERS tag/CTC/AgMNPs sensing platform with various concentrations of HepG2 (1-100 cells/mL) was shown in Figure 4b. The detection specificity is further evaluated by the spiking 50 HepG2, 100 MCF-7, and 100 L-02 cells in 1.0 mL of human blood sample respectively and the SERS signals was shown in Figure 4c. It is found that the SERS signal at 1331 $cm^{-1}$ is obvious for the HepG2 cells in the blood samples. However, for the MCF-7 and L-02 cells treated by the same operation, no corresponding SERS signal can be found. Consequently, it can be concluded that our system has a high specificity for HCC CTCs detection in the peripheral blood samples. To verify the selectivity furtherly, we supplment three other control human cancer cells, including HeLa, colon carcinoma (HCT116) and prostate (PC3) as a supporting information. The result was shown in Figure S6.

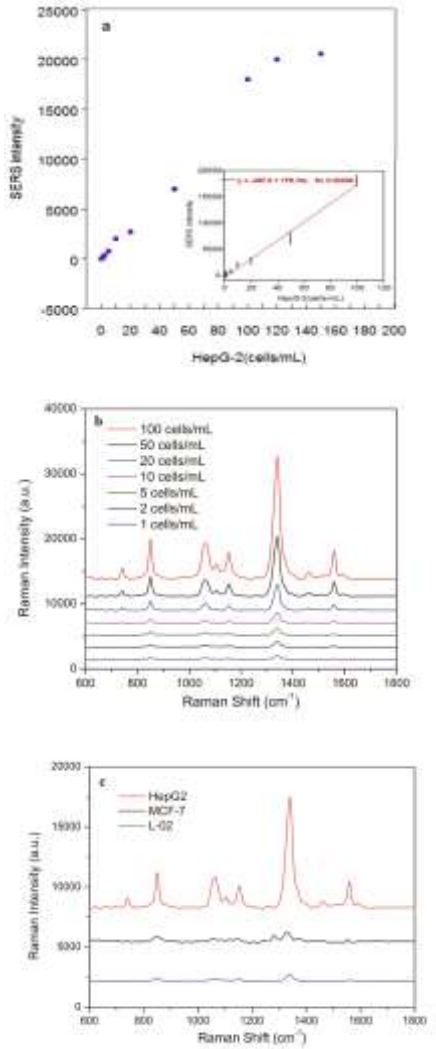


**Figure 4.** Detection sensitivity (a, b) and specificity (c) by the MNPs and SERS tag union for HepG2 cells in human peripheral blood: (a) SERS signals of blood sample (1.0 mL, ~0.5 × $10^7$ WBCs) with 1−150 HepG2 cells/mL after capture and labelling by the union; (b) the SERS spectra versus HepG2 cell concentration in the linear dependence; (c) SERS spectra of blood sample (1.0 mL, ~0.5 × $10^7$ WBCs) with 50 HepG2 cells, 100 MCF-7, and 100 L-02 cells treated by the same operation.

### Clinical applications

To demonstrate that the magnetic SERS nanoplatform can be used for liver cancer CTC analysis close to clinical settings, peripheral blood samples collected from 8 HCC patients, 3 breast cancer controls and 3 healthy controls were detected. Firstly, all the samples were incubed with anti-ASGPR-$Fe_3O_4$@Ag MNPs for HCC capture, after washing, the isolated cells were incubed with the anti-GPC3-Au@Ag@DTNB for labeling and SERS detection as described above. The result was provided in the table graph of Figure 5a. It showed that HCC CTCs could be detected in all the 8 blood samples from HCC patients and no identifiable HCC CTC was found in breast cancer patient and healthy samples. The SERS signal images of blood from patient #4(Liver cancer), #10(breast cancer), #14(healthy) was shown in Figure 5b, indicating this method is effective for detecting HCC CTCs with a small volume of blood sample (1-2 mL )with high specificity in clinical settings(low to 1 cell/mL).

a

| Sample No. | Cancer Type / Healthy | Gender | Volume Processed/mL | CTCs |
|---|---|---|---|---|
| 1 | Liver | F | 1.2 | 1 |
| 2 | Liver | F | 1.5 | 3 |
| 3 | Liver | F | 1.3 | 15 |
| 4 | Liver | M | 1.5 | 21 |
| 5 | Liver | M | 1.0 | 1 |
| 6 | Liver | F | 1.1 | 5 |
| 7 | Liver | F | 1.0 | 17 |
| 8 | Liver | F | 1.4 | 3 |
| 9 | breast | M | 1.2 | 0 |
| 10 | breast | M | 1.5 | 0 |
| 11 | breast | M | 1.0 | 0 |
| 12 | Healthy | F | 1.1 | 0 |
| 13 | Healthy | F | 1.3 | 0 |
| 14 | Healthy | M | 1.2 | 0 |

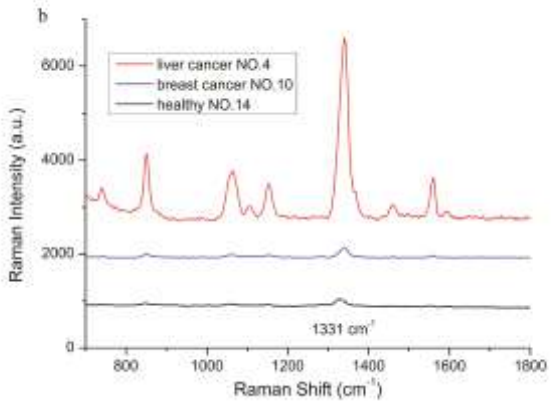


**Figure 5.** (a) Quantification of CTCs in blood samples from patients with liver cancers, breast cancers and healthy people.(b) SERS signals of blood from patient #4(Liver cancer), #10(breast cancer), and #14(healthy).

## Conclusions

In summary, we have designed a dual-enhancement SERS and dual-selective nanospheres system for rapid, efficient capture and sensitive detection of HCC CTCs. By the coupling of these antibody-nanopspheres, a good linear relationship ($R^2$ = 0.99) between the SERS intensity and the concentration of HCC CTCS in the range of 1−150 cells/mL can be observed with a LOD of 1 cells/mL. This system was successfully employed for detecting liver cancer patient peripheral blood samples. Until now, the EpCAM-IMNs based CellSearch system have only be applied to metastatic breast cancer, prostate cancer and colorectal cancer for clinical diagnosis with a 7.5 mL blood sample requirement. Therefore, our strategy can be used as a supplement for EpCAM- negative HCC CTC detection as the

operating steps was more convenient, rapid, and low-cost. We expect that the magnetic SERS based bioassay can also offer some ideas for the other types CTCs clinical diagnosis and biomedical research by changing the capture and labelling antibodies in the future.

## Experimental Section

### Materials and chemicals

Silver nitrate, ferric chloride ($FeCl_3.6H_2O$), ethylene glycol, formaldehyde (37%), and ammonia (28%) were purchased from Sinopharm Chemical Reagent Co. anti-GPC3 and anti-ASGPR antibodies were purchased from Beijing Biosynthesis Biotechnology Co., Ltd. 2-nitrobenzoic acid (DTNB), polyethyleneimine branched (PEI, MW 25 000), and polyvinylpyrrolidone (PVP, MW 40 000) were purchased from Sigma-Aldrich Chemicals Co. and all other chemicals were purchased from Shanghai Chemical Reagent Co., Ltd. Bovine serum albumin (BSA) was purchased from Invitrogen Biotechnology Co., Ltd. Human breast cancer cell line MCF-7, human HCC cell lines HepG2 and Human normal liver cell line L-02, human blood samples were obtained from 301 People's liberation army hospital. All the media used for cell culture were bought from Sigma-Aldrich Chemicals Co.

### Fabrication of $Fe_3O_4$@Ag core–shell MNPs and Au@Ag@DTNB NRs

The $Fe_3O_4$@Ag magnetic nanoparticles were synthetized as the method previous reported by our group. [27,28] Firstly, superparamagnetic $Fe_3O_4$ with a diameter of approximately 900 nm were synthesized. Then, cationic PEI self-assembled quickly on the $Fe_3O_4$ core to form a thin multifunction interlayer via sonication that can adsorb Au seed densely and uniformly and stabilize the entire structure. Then, $Fe_3O_4$@PEI-Au seed (10 mg) was dispersed in a silver nitrate aqueous solution (0.15 mM, 100 mL, with 0.2 wt% PVP), formaldehyde (37%, 150 mL) and ammonia solution (25%, 300 mL) was also added under sonication at 30 $^0$C within 2 min. Finally, the products were magnetically separated and rinsed five times with deionized water to remove the excess PVP. Au@Ag NRs were synthesized following the surfactant assisted, seed-mediated method reported in our previous papers. [22] Briefly, the AuNRs were synthesized through the Au seed solution and were purified and resuspended in a $AgNO_3$ solution to grow Ag shell. The prepared Au@Ag NRs were stirred with 10 μM DTNB under sonication for 1 h, the disulfide bond of DTNB can be quickly broken into thiol groups and be strongly bonded to the surface of Au@Ag NRs by the Ag-S bond. At the same time, as the free carboxyl end of the DTNB molecule, it was very convenient for subsequent antibody combining with the Au@Ag@DTNB through the coupling between of the amino of the antibody and the carboxyl of the DTNB.

### Fabrication of antibody conjugated $Fe_3O_4$@Ag MNPs and Au@Ag@DTNB NRs

Monoclonal anti-ASGPR and anti-GPC3 antibody were conjugated to the $Fe_3O_4$@Ag MNPs and Au@Ag@DTNB NRs respectively for the HCC isolation and SERS labeling in blood samples. For the one hand, the $Fe_3O_4$@Ag MNPs were incubated in an ethanolic solution containing 10 μM MUA and 10 μM MU for carboxyl decorating, then, the EDC/NHS carboxyl activation method was used to activate the carboxyl on the $Fe_3O_4$@Ag MNPs surface. The activated MNPs was incubated with a PBS solution (10 mM, pH 7.4) with 10 μg of ASGPR antibody at 4 °C overnight. After activation, the carboxyl on the $Fe_3O_4$@Ag MNPs can rapidly couple with amines of the ASGPR antibody. The unreacted carboxylgroups were blocked with 1% BSA solution for 2h and then washed twice with PBS and finally resuspended in PBS solution containing 1% BSA at 4 °C. For another, EDC (1 mM)/NHS (5 mM) were mixed with Au@Ag@DTNB NRs at 37 °C for 15min to activate the free carboxyl end of the DTNB, then 10 μg of GPC3 antibody were incubated with the Au@Ag@DTNB NRs in a PBS solution (10 mM, pH7.4) with at 4 °C overnight so that the carboxyl of the DTNB can rapidly couple with amines of the anti-GPC3 antibody. Finally, the unreacted carboxylgroups were blocked with 1% BSA solution for 2h and then washed twice with PBS and finally resuspended in PBS solution containing 1% BSA at 4 °C.

### Optimization of the dual-selective probes combination

Firstly, we tested the cell separation efficiency of the anti-GPC3 antibody-$Fe_3O_4$@Ag MNPs and anti-ASGPR antibody-$Fe_3O_4$@Ag MNPs by used an enzyme-linked immunosorbent assay (ELISA). We purchased the GPC3 ELISA kits from MSK Life Science Inc. Firstly, 50 μL anti-ASGPR (or GPC3)-antibody-$Fe_3O_4$@Ag MNPs with concentrations ranged from 0.1 mg/ mL to 0.6 mg/ mL was incubated with infected human blood containing $2 \times 10^3$ HepG2 tumor cells in 2 mL suspensions of citrated whole human blood for 30 min with gently shaking. Next, a magnet was used to separate the HepG2 tumor cells attached on the surface of the MNPs. Finally, the amount of GPC3 levels in the captured cells was detected by the GPC3 ELISA kits accordance with the manufacturer's instructions. For the control, unmodified $Fe_3O_4$@Ag MNPs were used for HepG2 tumor cells separating in the same conditions. Secondly, 3 kinds of combinations: anti-ASGPR-MNPs/ anti-ASGPR-SERS tag (group 1), anti-ASGPR-MNPs/anti-GPC3-SERS tag (group 2), anti-GPC3-MNPs/anti-GPC3-SERS tag (group 3), MNPs/SERS tag (control) (50 μL, 0.5 mg/mL) were incubated with the same whole human blood samples with same HCC tumor spiked cells(1.0 mL, ～100 CTCs) , after magnetic separation and SERS tag labelling, the 3 samples were washed and resuspended in a PBS solution for the further testing by the Raman instrument.

### Cell separation specificity and cell viability study

To demonstrate the specificity of the capture probes, after the capture by the anti-ASGPR antibody-$Fe_3O_4$@Ag MNPs, we also used Alexa488-GPC3 antibodies for HCC cells captured previous staining for 30 min at 37 °C. After that, cell specimen was observed under an inverted fluorescence microscope and only HepG2 tumor cells were positive to the Alexa488-GPC3 antibodies to laser green fluorescence. To study the cell viability, calcein AM and propidium iodide (PI) were used to stain the isolated tumor cells to analyze their viability. Calcein AM can penetrate the live cell membrane and react with the intracellular esterase to form calcein with green fluorescence, while PI is a membrane-impermeable nuclear stain that can stain only dead cells, resulting in red fluorescence. [29,30] The recovered cells were stained with 2 μM calcein AM and 4 μM PI for 30 min at 37 °C and the viability was examined. Furthermore, to determine whether the isolated cells can be directly recultured and propagated in vitro, the recovered HCC cells were recultured in a 96-well plate.

**Sensitivity and specificity assay**

To study the sensitivity of the nanoparticles system, HCC tumor cells (initial concentration $1\times10^5$ cells/mL in 1×PBS) were spiked in citrated whole human blood (1 mL) at various densities. Next, anti-ASGPR conjugated $Fe_3O_4$@Ag MNPs (50 μL, 0.5 mg/mL) were mixed with the infected blood for 30 min at room temperature before the magnetic separation experiment was performed. After magnetic separation and washing, the recovered cells were resuspended in a BBS solution, anti-GPC3 antibody conjugated Au@Ag@DTNB (50 μL, 0.3 mg/mL) were added to the solution and cultured in a 37°C incubator. After 30 min of incubation, the sample was washed and resuspended in a PBS solution for the further testing by the Raman instrument. To study the specificity of the assay, a similar protocol was performed except for only one different point, which is that the MCF-7 human breast cancer cells, L-02 Human normal liver cell, HeLa, colon carcinoma (HCT116) and prostate (PC3) were added into the citrated whole human blood and mixed with the two antibody conjugated nanoparticles for magnetic isolation and SERS detection.

**CTCs detection in HCC patient peripheral blood samples**

We collected 18 whole blood samples including 8 liver cancer patients, 5 breast cancer patients and 5 healthy people from 301 People's liberation army hospital. The samples were incubated with the anti-ASGPR-$Fe_3O_4$@Ag MNPs and then the isolated cells were incubated with the anti-GPC3-Au@Ag@DTNB for SERS detection as described above.

## Acknowledgements

This work was supported by Grants from the National Natural Science Foundation of China (No. 81702106), Beijing Municipal Science & Technology Commission (No. Z161100000116040).

**Keywords:** Surface-enhanced Raman scattering (SERS) • Hepatocellular carcinoma • Circulating tumor cells • Dual-selective • Dual-enhanced SERS

[1] C. Aggarwal, N. J. Meropol, C. J. Punt, N. Iannotti, B. H. Saidman, K. D. Sabbath, N. Y. Gabrail, J. Picus, M. A. Morse, E. Mitchell, M. C. Miller, S. J. Cohen, *Ann. Oncol.* **2013**, *24*, 420–428.

[2] M. Cristofanilli, T. Budd, M. J. Ellis, A.Stopeck, J. Matera, C. Miller, J. M. Reuben, G.V. Doyle, W. J. Allard, L. Terstappen, D. F. Hayes, *Engl. J. Med.* **2004**, *351*, 781-791.

[3] T. Yamashita, M. Forgues, W. Wang, J. W. Kim, Q. Ye, H. Jia, A. Budhu, K. A. Zanetti, Y. Chen, L. X, Qin, Z. Y. Tang, X. W. Wang, *Cancer Research* **2008**, *68*, 1451-1461.

[4] M. Yu, S. Stott, M.Toner, S.Maheswaran, D. A. Haber, *J. Cell Biol.* **2011**, *192*, 373–382.

[5] F.B. Wang, Y. Rong, M. Fang, J.P. Yuan, C.W. Peng, S.P. Liu, Y. Li, *Biomaterials* **2013**,*34*, 3816-3827.

[6] X. P. He, B. W. Zhu, Y. Zang, J. Li, G. R. Chen, H. Tian, Y. T. Long, *Chem. Sci.* **2015**, *6*, 1996-2001.

[7] M. Kalinich, I. Bhan, T. T. Kwan, D. T. Miyamoto, S. Javaid, J. A. LiCausi, J. D. Milner, X. Hong, L. Goyal, S. Sil, M. Choz, U. Ho, R. Kapur, A. Muzikansky, H. Zhang, D. A. Weitz, L. V. Sequist, D. P. Ryan, R. T. Chung, A. X. Zhu, K. J. Isselbacher, D.T. Ting, M. Tonere, S. Maheswaran, D. A. Haber, *PNAS* **2017,** 114, 1123-1128.

[8] R. Konigsberg, E. Obermayr, G. Bises, G. Pfeiler, M. Gneist, F. Wrba, M.de Santis, R. Zeillinger, M. Hudec, C. Dittrich, *Acta Oncol.* **2011**,*50* 700-710.

[9] B. S. Desitter, N. Guerrouahen, J. Benali-Furet, P.A. Wechsler, Y. Janne, M. Kuang, L. Yanagita, J.A. Wang, R.J. Berkowitz, Y.E. Distel, *Anticancer Res.* **2011**,*31* 427-441.

[10] R.L. Eifler, J. Lind, D. Falkenhagen, V. Weber, M.B. Fischer, R. Zeillinger, *Cytometry Part B: Clin.Cytometry* **2011**,*80* ,100-111.

[11] W. Xu, L. Cao, L. Chen, J. Li, X.F. Zhang, H.H. Qian, X.Y. Kang, Y. Zhang, J. Liao, L.H. Shi, Y.F. Yang, M.C. Wu, Z.F. Yin, *Clin. Cancer Res.* **2011** *17,* 3783-3793.

[12] Y. L. Shi, A. Pramanik, C. Tchounwou, F. Pedraza, R. A. Crouch, S. R. Chavva, A. Vangara, S. S. Sinha, S. Jones, D. Sardar, C. Hawker, P. C. Ray, *ACS Appl. Mater. Interfaces.* **2015**,*7*,10935-10943.

[13] L. Chen, L. Wu, Z.L. Zhang, J. Hu, M. Tang, C.B. Qi, N. Li, D.W. Pang, *Biosens bioelectron* **2016**,*85*,633-640.

[14] D. Tsoutsi, J. M. Montenegro, F. Dommershausen, U. Koert, L. M. Liz-Marzán, W. J. Parak, R. A. Alvarez-Puebla, *ACS Nano.* **2011**,*5* ,7539-7546.

[15] Y. Wang, B. Yan, L. Chen, *chem. Rev.* **2013**,*113*, 1391−1428.

[16] D. Li, Y. Zhang, R. Li, J. Guo, C. Wang, C. Tang, *Small* **2015**,*11*, 2200-2208.

[17] Y. C. Chang, C. Y. Yang, R. L. Sun, Y. F. Cheng, W. C. Kao, P. C. Yang, *Sci. Rep.* **2013,** *3*,1863.

[18] X. Wu, L. Luo, S. Yang, X. Ma, Y. Li, C. Dong, Y. Tian, L. Zhang, Z. Shen, A. Wu*, *ACS Appl. Mater. Interfaces.* **2015**, *7*, 9965-9971.

[19] P. Zhang, R. Zhang, M.Gao, X. Zhang, *ACS Appl. Mater. Interfaces* **2014**, *6*, 370-376.

[20] Z. A. Nima, M. Mahmood, Y. Xu, T. Mustafa, F. Watanabe, D. A. Nedosekin, M. A. Juratli, T. Fahmi, E. I. Galanzha, J. P. Nolan, A. G. Basnakian, V.P. Zharov, A. S. Biris, *Sci. Rep.* **2014**,*4* ,4752.

[21] J.F. Wang, X. Wu, C. Wang, Z. Rong, H.Ding, H.Li, S. Li, N. Shao, P. Dong, R. Xiao, S. Wang, *ACS Appl. Mater. Interfaces.* **2016**, *8,* 19958-19967.

[22] R. Zhen, J.F. Wang, C. W. Wang, R. Xiao, S. Q. Wang, *Biosens bioelectron* **2016**,*84*,15-21.

[23] Y. Xiang, X. Wu, D. Liu, Z. Li, W. Chu, L. Feng, K. Zhang, W. Zhou, S. Xie, *Langmuir* **2008**,*24*,3465-3470.

[24] J. Zhang, L.L. Cao, W. Xu, Z. Yin, *Semin. Oncol.* **2012***, 39*, 449-460.

[25] L. J. Wu, Y. D. Pan, X. Y. Pei, H. Chen, S. Nguyen, A. Kashyap, J. Liu, J. Wu, *Cancer Lett.* **2012**,*326*,17-22.
[26] B. P. V. Nellore, R. Kanchanapally, A. Pramanik, S. S. Sinha, S. R. Chavva, A. Hamme, P. C. Ray, *Bioconjugate Chem.* **2015**, *26*,235-242.
[27] J.F. Wang, X. Wu, C. Wang, Z. Rong, H. Ding, H. Li, S. Li, N. Shao, P. Dong, R. Xiao, S. Wang, *ACS Appl. Mater. Interfaces.* **2015**,*7*, 20919-20929
[28] C.W. Wang, J.W. Xu, J.F. W, R. Zhen, L. Ping, R. Xiao, S.Q. Wang, *J. Mater. Chem. C.* **2015,***3*,8684-8693.
[29] S. Nagrath, L. V. Sequist, S. Maheswaran, D. W. Bell, D. Irimia, L. Ulkus, M. R. Smith, E. L. Kwak, S. Digumarthy, A. Muzikansky, *Nature* **2007**,*450*,1235-1239.
[30] B. D. Plouffe, M. Mahalanabis, L. H. Lewis, C. M. Klapperich, S. K. Murthy, *Anal. Chem.* **2012**,*84*,1336-1344.
[31] C.L. Sun, R. Zhang, M.X. Gao, *Anal bioanal chem* **2015**,*407*, 8883-8892.
[32] X. Wu, L.Q. Luo, S. Yang, X. H. Ma, Y. l. Li, D. Chen, Y.C. Tian, L. Zhang, Z. Shen, A.G. Wu, *ACS Appl. Mater. Interfaces.* **2015**,*7*,9965-997

10.1002/chem.201801133